Fracture in Monolithic Ceramics at High Temperatures

RISHI RAJ

Department of Materials Science and Engineering, Bard Hall Cornell University, Ithaca, New York 14853-1501, USA

ABSTRACT

Failure prediction in monolithic structural ceramics has generally been modelled in terms of crack propagation, by invoking the mechanism of the growth of cavities and microcracks at grain interfaces. The discussion in this paper is based on the premise that realistic design of engineering components from monolithic ceramics requires a threshold criterion for failure. A threshold criterion is derived and expressed in terms of a Mode I stress intensity factor or a uniaxial stress, assuming a design life of 30 years. The criterion relies on the condition for damage initiation, where damage is defined to be the cavities that form at grain boundaries at high temperatures. This visualization of damage allows the incorporation of microstructural parameters in the analysis, such as the grain size, the viscosity and the volume fraction of a glass that may be present at grain interfaces, and the dihedral angles associated with grain boundaries. Experiments that can lead to a measurement of the threshold values are suggested.

KEYWORDS

Ceramics; High Temperature Fracture; Threshold Stress Intensity Factor; Cavities; Nucleation; Creep Damage; Silicon Nitride; Creep Crack Growth

INTRODUCTION

Ceramics are unconventional materials for high temperature structural applications. In comparison to metals, they are much harder and melt at far higher temperatures. The highest service temperature of modern nickel-base superalloys is less than 1300 K; which equals 0.75 of the melting point of nickel. In contrast the sublimation temperature of silicon nitride or silicon carbide is approximately 3000 K, which extrapolates to a possible service temperature that is twice that of the superalloys if scaled in a similar way. The density of ceramics, which is nearly one third the density of nickel-base alloys, makes ceramic materials even more attractive for high temperature applications.

The technological development of structural ceramics is limited by two factors. One relates to the processing of ceramics into shapes that have reliable mechanical properties. The second issue is the ability to predict the long term mechanical properties in terms of parameters that can be used in engineering design. Both issues are interrelated through the microstructure. The processing determines the microstructure, which then controls the mechanical properties of the material.

Structural ceramics can be monolithic or they can be fiber reinforced. While the composites offer outstanding opportunities, their development awaits the availability of ceramic fibers that can withstand the very high temperatures required in processing composites. The fundamental understanding of the mechanical properties of composites presents issues that can be different than those arising in the case of monolithic ceramics. For example, the orientation of the fibers and their ability to arrest crack propagation are probably not so important in developing life prediction models for monolithic ceramics. However, the knowledge gained from the monoliths, for example the role of grain interfaces in the fracture process, can be useful in failure prediction of composites. The present discussion is limited to monolithic ceramics.

In approaching the issue of life prediction for ceramics, we seek, first, to identify the phenomenological parameters that can be used in the engineering design of components. The typical creep curve has the form illustrated in Fig. 1, when the test is carried out by applying a fixed, uniaxial, tensile

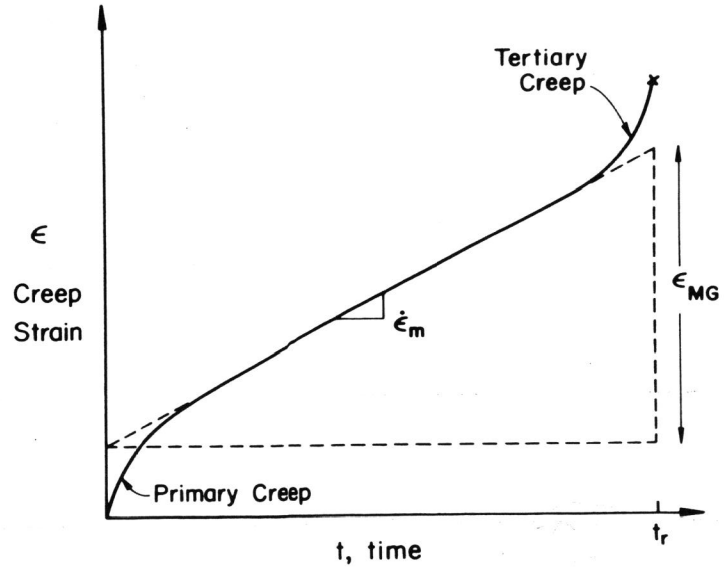

Fig. 1. Typical creep curve in a creep rupture experiment, $\dot{\epsilon}_m$ is the minimum creep rate, and t_r is the time to rupture. Note the accelerated creep rate near fracture, known as tertiary creep. The experiment is carried in tension with dead weight loading.

load to the specimen. In the metallurgical literature this test is known as creep rupture. The minimum creep rate, $\dot{\epsilon}_m$, and the time to failure, t_r, are measured. Their product, ϵ_{MG}, is given by the Monkman Grant equation:

$$\dot{\epsilon}_m t_r = \epsilon_{MG} \tag{1}$$

It is found that ϵ_{MG} is often independent of stress and temperature. Representative data for polycrystalline alumina are given in Fig. 2 (Davies and Ray, 1972). The data span two orders of magnitude in strain rate and 200 K in temperature. It yields a reasonably constant value for ϵ_{MG} that is equal to 1.5%. Similar experiments on vitreous bonded aluminum oxide carried out by Wiederhorn et al. (1986), yielded a Monkman Grant ductility of only 0.04%. In comparison the values for ϵ_{MG} in stainless steels and nickel-base superalloys range from 1% to 20%.

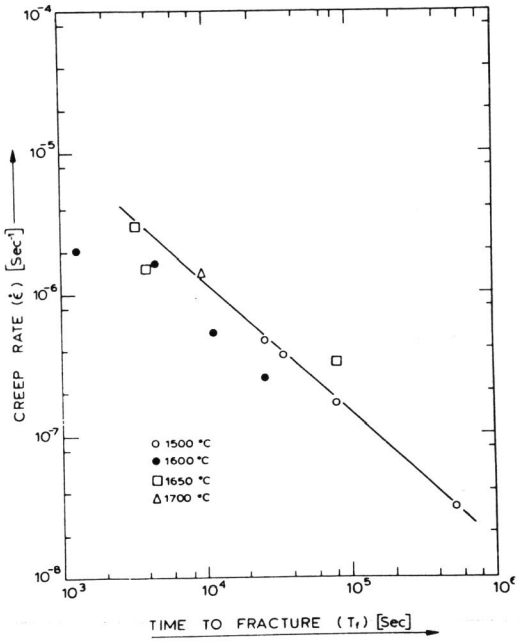

Fig. 2. A Monkman Grant plot for tensile creep rupture experiments in alumina. Note that Eq. (1) is satisfied by the inverse linear slope between log ($\dot{\epsilon}_m$) and log (t_r); and that $\epsilon_{MG} \cong 1.5\%$ (Davies and Ray, 1972).

Structural components made from stainless steels and nickel-base superalloys are designed on the basis of creep rupture life, t_r. The thirty year life is extrapolated from:

$$t_r = \frac{A}{\sigma^n} \tag{2}$$

where σ is the tensile stress and n is the power law stress exponent; A is microstructure and temperature dependent. Because of the constraint imposed by Eq. (1), n is also the stress exponent for the creep rate, $\dot{\epsilon}_m$. The design codes require a safety factor on the stress values extrapolated from Eq. (2).

The design code prescribed by the engineers, and the phenomenological relationship between creep rate and fracture time given by Eq. (1) have guided the development of new metallic alloys. The emphasis has been placed upon increasing the creep resistance of the alloys. That lowers $\dot{\varepsilon}_m$, and, as a consequence of Eq. (1) enhances longevity. Eventually this approach has reached its own limits. As the nickel-base superalloys have become harder their mode of failure has shifted from extensive damage to local damage near crack tips. The change to crack initiation and propagation mode of failure has led to a fracture mechanics approach to failure prediction. Loading parameters that account for enhanced plasticity near the crack tip (Riedel, 1985) and those which invoke linear elastic fracture mechanics (Pineau, 1985) have been proposed. Experimental work on creep crack growth in one alloy is described in detail in Ref. (Sadananda and Shahinian, 1977). In general, as the Monkman Grant ductility becomes smaller the probability of crack initiation and propagation mode of failure increases. The micrographs in Fig. 3 contrast the extensive damage in the polycrystalline alumina sample (Davies and Ray, 1972), where ε_{MG} was equal to 1.5%, with the crack growth failure in the vitreous alumina sample (Wiederhorn et al., 1986), where ε_{MG} is only 0.04%.

EXTENSIVE CAVITATION DAMAGE

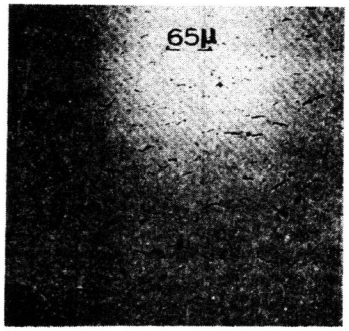

Alumina

CRACK PROPAGATION

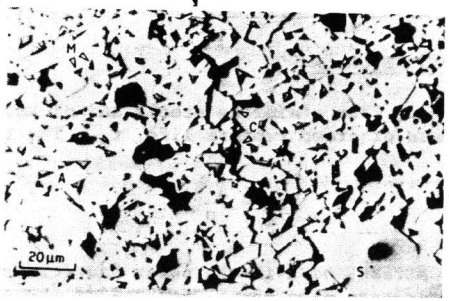

Vitreous Bonded Alumina

Fig. 3. Micrographs of failure by extensive damage (Ref. 1) and by crack propagation (Ref. 2). The tensile axis is vertical.

The most recent design rules for structural components (ASME: Interpretations of the ASME Boiler and Pressure Vessel Codes, Case 1592, American Society for Mechanical Engineers, New York, 1974), 1974) implicitly recognize the difficulty of applying Eq. (2) when fracture occurs with very low ductilities. The code prescribes that the design stress must be the least of (i) two-thirds of the minimum stress to cause creep rupture, or (ii) 80% of the minimum stress to cause onset of tertiary creep, or (iii) the minimum stress to cause a total creep strain of 1%. While these criteria can still be applied to relatively ductile materials such as stainless steels and the earlier nickel-base superalloys, the new superalloys are extremely creep-brittle, and as a result, would have difficulty in meeting the third criterion just mentioned. Ceramic materials are even more creep resistant than the nickel-base superalloys. Thus a fracture mechanics approach to failure prediction in ceramics appears more suitable than the Monkman Grant approach. Such an approach is also needed because processing defects, that occur in sintered materials (Evans, 1982), often serve as sites for failure initiation. The fracture mechanics methodology allows consideration of these flaws in evaluating the risk of life prediction.

In the following sections, we first describe the metallographic observations and the phenomenological measurements of fracture in ceramics, principally silicon nitride. These data lead to the inference that measurements of a threshold stress intensity factor should be sought for life prediction under service conditions. In the next section models that are able to give a micromechanical basis to the threshold are described. At the end, experiments which reflect on the validity of specific physical models, and on the fracture criterion under multiaxial loading, are discussed. Finally, a fresh approach for further fundamental experimental work is suggested.

CHARACTERISTICS OF FRACTURE IN POLYCRYSTALLINE CERAMICS AT HIGH TEMPERATURE

High temperature fracture in ceramics is invariably intergranular. It is suspected that the microscopic damage that causes fracture consists of small cavities that form at grain boundaries. Since the grain size in ceramics is often small, the cavities only have to grow to be about one micrometer before they link with their neighbors and cause total separation. While the small cavities themselves have been seen in only very few studies, separated grain facets are often observed. A striking example of profuse intergranular fracture in alumina is shown in Fig. 4 (Kingery et al., 1976). The very small cavities which link to create the microcracks can be seen if the grain size is large; an example is given in Fig. 5 where cavities have formed on planes which are parallel to the compression axis (Poteat and Yust, 1966). (Later, it will be argued that cavities grow on those grain boundaries that are aligned for the maximum principal stress; the observation in Fig. 5 agrees with this criterion.)

In the examples described just above, cavities form extensively throughout the specimen. Intergranular fracture can also occur by the propagation of a single intergranular crack, without any ostensible cavitation damage. In some instances microcracks can be seen elsewhere in the specimen even when the propagation of one predominant crack has caused the fracture. These observations, then, suggest three possible types of fracture processes:

A. Extensive damage at grain boundaries.
B. Initiation and propagation of an intergranular crack by the growth of localized damage near the crack tip.
C. Stress corrosion crack propagation.

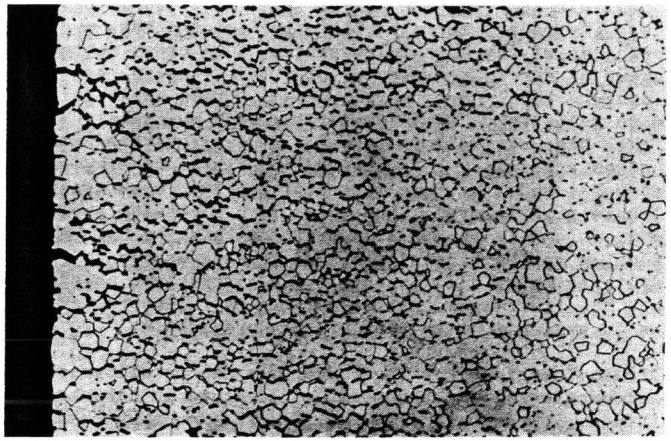

Fig. 4. Extensive creep damage in polycrystalline alumina deformed in four point bending at high temperature (courtesy Introduction to Ceramics, W. D. Kingery, H.K. Bowen and D.R. Uhlmann, J. Wiley & Sons, NY, 1976, p. 808).

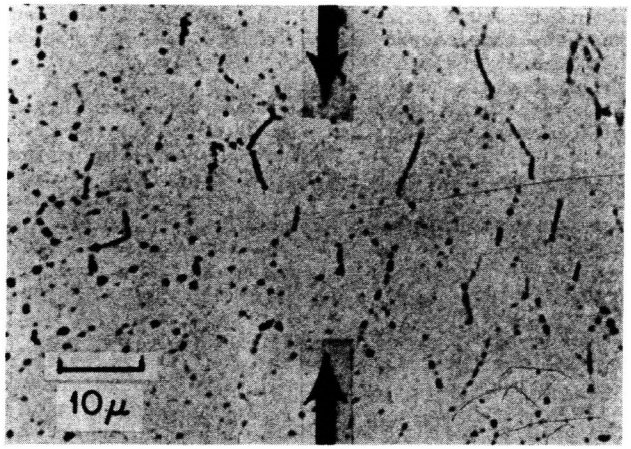

Fig. 5. Nucleation of small cavities in ThO2 on those grain boundary planes that are oriented for the maximum principal stress (Poteat and Yust, 1966).

Failure prediction methods that are most likely to be adopted in engineering design are based on simple equations. Equation (2) illustrates a one parameter approach to extrapolation of creep rupture data to design conditions (based upon the power stress exponent). While Eq. (2) is appropriate when fracture takes place by the extensive damage process, crack propagation failure is often characterized by the following equation:

$$\dot{a} = BK_I^p \tag{3}$$

where $\dot{a}$ is crack propagation velocity, B is a temperature and microstructure dependent parameter, K_I is the mode I stress intensity factor, and p is stress-intensity exponent. The validity of life prediction, using either Eq. (2) or Eq. (3) depends upon the reliability of the exponents n and p. Discussion of the fracture and the deformation mechanisms (Nix and Gibeling, 1985; Frost and Ashby, 1982; Gandhi, 1985) shows that, in metals, n changes when the mechanism of the deformation and the fracture, changes. Thus, caution is needed when extrapolating laboratory data to predict service life.

The uncertainty in the prediction of fracture behavior on the basis of Eq. (3) was recognized by Pletka and Wiederhorn (1982) who found that the method applied only in simple materials such as glass and one glass ceramic. Procedures for proof testing that start with the assumption of Eq. (3) have also been developed (Ritter et al., 1980; Fuller et al., 1980), but have been found difficult to implement because of time dependent changes in the flaw populations due to environmental degradation, especially in silicon nitride (Wiederhorn and Tighe, 1983).

In view of the preceding discussion we search for an alternative to Eq. (3) for life prediction. We begin by studying the observations that have been made in the studies of high strength nickel-base superalloys. A typical set of data, taken from Sadananda and Shahinian (1977) is shown in Fig. 6. It shows two regions of behavior: at low K_I the crack growth rate increases rapidly with K_I but then less rapidly as K_I is increased further. Data obtained from different specimen geometries show some scatter but appear to converge at small values of K_I. The very interesting point is that the higher slope dominates at the lower values of K_I; if the two slopes were a result of two different mechanisms that contributed additively to crack growth, then the lower slope would have dominated at the lower values of K_I. The implication is that crack growth occurs not by two additive mechanisms but by two sequential steps, each of which is necessary for the growth of the crack. Later we will interpret this behavior in terms of the nucleation and growth of cavities in front of the crack tip, where the threshold like behavior at low K_I's becomes limited by cavity nucleation.

It is interesting to compare the data in Fig. 6 with the data for stress corrosion cracking in soda lime glass (Wiederhorn, 1967). In that case damage is induced not by cavitation but by the humidity in the environment that weakens the crack tip. Still, the data resemble those for the high temperature growth in superalloys; except that the threshold moves to lower stress intensities as the humidity is increased.

The discussion presented above prompts us to propose a general form for crack propagation behavior in ceramics at high temperature. It is presented in Fig. 7, and consists of three Stages. The slope p_{II} in Stage II is smaller than in either Stage I or Stage III. We assume that Stage I ap-

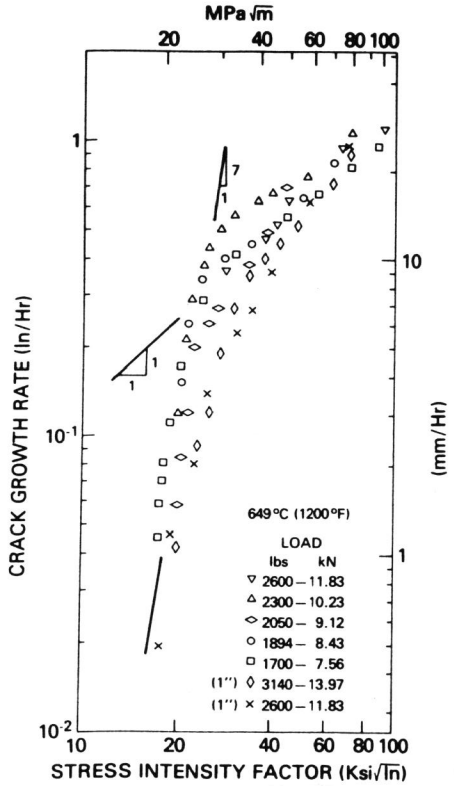

Fig. 6. Creep crack growth data in a Ni-base superalloy (Sadananda and Shahinian, 1977).

proaches a threshold in an asymptotic way; as a result the slope p_I is expected to increase as K_I decreases. The effective threshold is defined by the design life of 30 years = 10^9 seconds. Laboratory measurement of the threshold would require a crack propagation rate sensitivity of 10^{-10} cm s^{-1} assuming that fracture occurs when a crack grows to a length of 1 mm. Because of the high slope p_I, large variations in crack propagation rate amount to only small change in K_I; therefore, a small safety factor in K_I can allow extrapolation of cracking propagation rate over several orders of magnitude with good confidence. This point has been discussed by Wiederhorn et al. (1976). Effectively, therefore, a measurement sensitivity of about 10^{-6} cm s^{-1} in the laboratory should suffice for reliable prediction of the effective threshold.

While a great deal more experimental work is needed on threshold behavior in ceramics at high temperatures, a few studies in the literature support the idea that a true threshold does in fact exist. Karunaratne and Lewis (1980) provide mechanical as well as photographic evidence of the existence of a threshold in polycrystalline SiAlON. The threshold appears to occur because

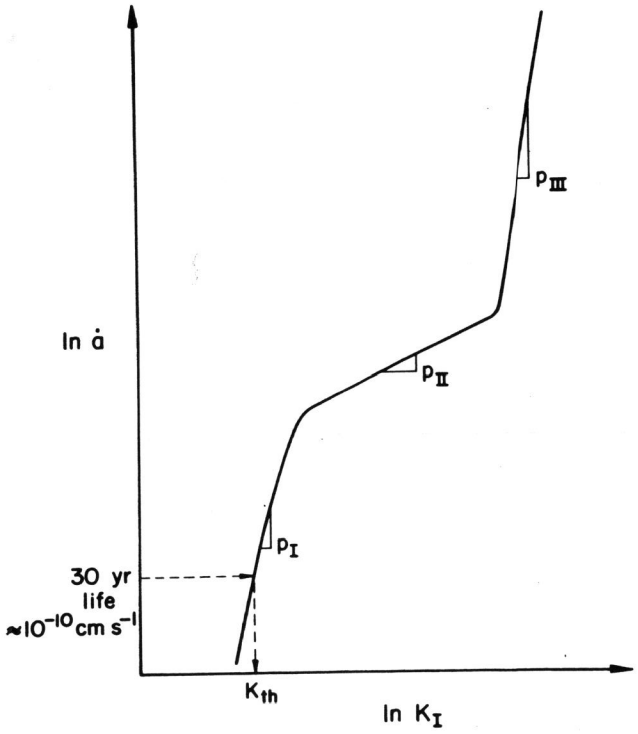

Fig. 7. Assumed form of crack propagation behavior in monolithic structural ceramics at high temperature.

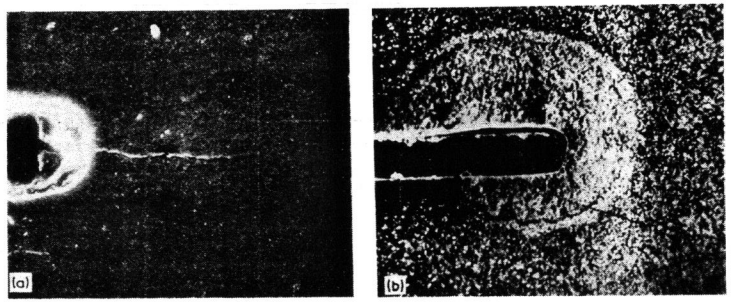

Fig. 8. Evidence of crack propagation above, and crack arrest below a critical value of the stress intensity factor, in SiAlON (Karunaratne and Lewis, 1980).

of competition between rate of crack propagation and the rate of the relaxation of stress near the crack top by diffusional creep mechanisms. Below a critical threshold, the stress relaxation is faster and the crack does not grow. The picture in Fig. 8 shows a relaxation zone that forms when K_I is below a critical value. The evidence of superplasticity in ceramic materials (Venkatachari and Raj, 1986) gives further support to the possibility of crack blunting by creep, leading to the existence of a threshold. Minford and Tressler (1983) report a threshold in SiC and attribute it to creep relaxation or oxidation induced blunting of the crack tip. Wiederhorn and Tighe (1983) report amelioration of pre-existing flaws in specimens of silicon nitride in long term testing, and attribute it to oxidation and creep relaxation.

Finally, the diagram in Fig. 7 was suggested by McHenry and Tressler on the basis of their experiments with silicon carbide (McHenry and Tressler, 1980). A transition from Stage II to Stage III fracture in silicon-nitride was reported by Evans and Wiederhorn (1974).

In the next section a theoretical approach to the possible existence of a K_{th} is presented.

MODELS FOR THRESHOLD BEHAVIOR IN STRUCTURAL CERAMICS AT HIGH TEMPERATURE

The papers (Karunaratne and Lewis, 1980; Minford and Tressler, 1983) summarized in the previous section suggest that oxidation, and creep relaxation play a role in defining a threshold stress intensity. Oxidation can blunt the crack but we must include the possibility that it can also cause stress corrosion type of crack growth, essentially similar to the stress corrosion cracking in glass at ambient temperature (Wiederhorn, 1967). Similarly, creep relaxation can blunt the crack tip but it can also produce cavitation damage at grain interfaces as discussed earlier. The theoretical study of the threshold is therefore complex, involving several competing processes. At this stage we approach the problem with simplifications that make it tractable.

The approach proposed here requires the following assumptions: (i) Deformation is linear elastic except for the growth of cavities at grain boundaries that can occur by diffusional transport or by viscous flow. (ii) The crack tip remains sharp and is not relaxed by oxidation or by pure shear creep deformation; however, the model recognizes that the local stress distribution can change as a result of the nucleation and growth of intergranular cavities near the crack tip. (iii) Nucleation and growth of cavities is the principal mechanism of crack propagation.

The model is presented schematically in Figs. 9 and 10. The crack is assumed to propagate by the formation of microcracks ahead of the crack tip as shown in Fig. 9a. Each of these microcracks is assumed to nucleate in the form of cavities at triple grain junctions as illustrated in Fig. 9c. To simplify the analysis we assume the cavities to lie on a single plane in front of the crack tip at a distance equal to the grain size, d, from each other, as shown in Fig. 9b.

The crack propagation problem reduces to the analysis of conditions under which cavities can continue to nucleate (Raj, 1978; Tsai and Raj, 1982) in front of the crack tip, and then grow to the point where they can link with, and advance the crack tip. If the partial growth of cavities depresses the

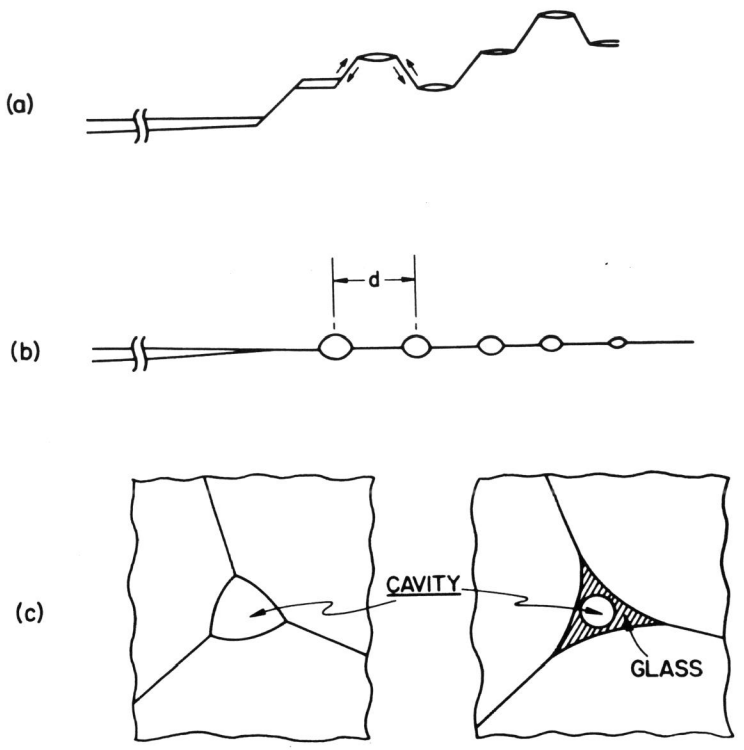

Fig. 9. Idealization of the fracture mechanism where crack propagation occurs by the nucleation of cavities ahead of the crack tip. (a) Crack propagation by grain boundary microcracks. (b) The problem above is analyzed in the terms of the nucleation of each of the microcracks in the form of small cavities that are placed a grain size apart on a planar boundary. (c) The nucleation of cavities in triple grain junctions when the polycrystal does not contain an intergranular glass and when it does.

stress distribution in front of the crack tip to the extent that the principal stress everywhere becomes less than the nucleation stress, then the crack will not grow. This condition of loading then prescribes the threshold stress intensity factor. The concept is illustrated schematically in Fig. 10. In the absence of cavities the stress distribution ahead of the crack is obtained from linear elastic fracture mechanics. Since that stress is greater than the threshold stress for cavity nucleation, δ_{th}, a cavity will nucleate in front of the crack tip at the nearest triple grain junction. As that cavity grows it will relax the stress distribution, as shown. The stress will change further as more cavities are nucleated. If a situation is reached that the stress relaxes to less than δ_{th} everywhere, before the crack tip can link with the first cavity, then the crack will be arrested; this condition, which is illustrated at the bottom of the schematic in Fig. 10, prescribes K_{th}.

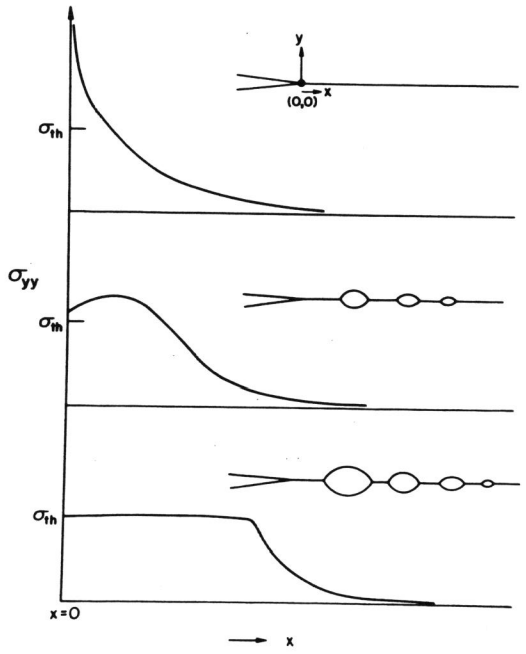

Fig. 10. The change in the tensile stress in front of the crack tip when cavities nucleate at triple grain junctions. A stress that is greater than $\hat{\sigma}_{th}$ is required. If the crack does not move forward when the stress ahead of the crack tip is greater than $\hat{\sigma}_{th}$, then the crack is arrested. The transition condition, illustrated by the schematic at the bottom defines the threshold stress intensity factor.

The problem illustrated in Fig. 10 has been analyzed in detail by Raj and Baik (1980). The result given by their equation 28 is reproduced here with new nomenclature:

$$K_{th} = \sqrt{\alpha d E \hat{\sigma}_{th}} \qquad (4)$$

where K_{th} is the threshold stress intensity factor, d is the cavity spacing which is assumed equal to the grain size, E is the Young's Modulus of the material, and $\hat{\sigma}_{th}$ is the maximum principal stress required for cavity nucleation (this is discussed further later). The parameter α is a geometrical parameter which takes into account the shape of the cavity. It prescribes how much material must be displaced so that adjacent cavities grow to a size where they can touch. For a single phase material $\alpha = 0.4$ if the included angle for the lenticular shaped cavity is 150°. In the general case it would be reasonable to assume that α lies in the range of 0.1 to 0.5.

The use of grain size to prescribe the cavity spacing in Eq. (4) needs to be discussed further.

We move now to discuss $\hat{\sigma}_{th}$. This parameter depends on the structure of the grain boundaries. We consider the case where a small amount of glass phase is segregated at the grain boundaries. The glass is often a silicate or an oxynitride, and its presence arises from the use of sintering additives that are required to enhance matter transport along the grain boundaries, especially in covalent materials such as silicon nitride. The glass can also form inadvertently because silica forms deep eutectics with many oxides, and because silica is a common impurity acquired from the environment during processing. The volume fraction of the glass, and how it is distributed at the grain boundaries has been addressed by Raj (1981); there it was shown that (i) the glass forms an interconnected network when the dihedral angle it forms at triple grain junctions is less than $\pi/3$, and (ii) the majority of the glass is segregated to triple grain junctions. The volume fraction of the glass, v_g, is uniquely related to the grain size, d, the dihedral angle, and the radius of the interstitial unit that just fits in the triple grain junction. The geometry is illustrated in Fig. 11. For the perfectly wetting case, that is when the dihedral angle is zero, this relationship is as follows:

$$v_g = \frac{17\, u^2}{d^2} \qquad (5)$$

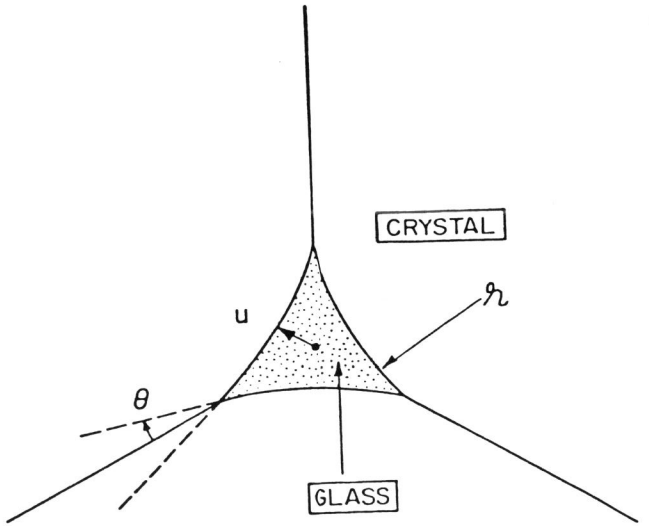

Fig. 11. The geometrical parameters which define the distribution of the glass at grain boundaries of a polycrystal (Raj, 1981).

As an illustration, if the polycrystal contains 5 volume % glass and its grain size is 1 μm then radius of the glass pocket at triple junctions will be 50 μm, according to Eq. (5).

The nucleation stress for polycrystals that contain fluid phase has been considered by Tsai and Raj (1982), and leads to the following result:

$$\sigma_{th} = \frac{4.2\ \gamma_g}{d\sqrt{v_g}} \qquad (6)$$

Here, γ_g is the surface tension of the fluid. Equation (6) is derived on the basis that the critical nucleus size is determined by the size of the fluid pocket that fills the triple grain junctions; it assumes that Eq. (5) represents the relationship between the critical size and the volume fraction. More detailed analysis of cavity nucleation in such microstructures is given by Marion et al. (Marion et al., 1983).

Equation (6) gives the interesting result that cavities would be more difficult to nucleate if the volume fraction of the fluid is smaller; this is contrary to intuitive reasoning which would suggest that a greater amount of the fluid in the polycrystal will lessen the probability of fracture. Experimental work by Lange et al. (Lange et al., 1980), however, is in agreement with Eq. (6); they found that increasing the volume fraction of the fluid from 4% to 17% increased the rate of cavitation more than twenty times.

Finally, we discuss the nucleation stress for cavitation in ceramic polycrystals that do not contain a liquid phase (Raj, 1978). Here, the magnitude of the stress depends on the site of nucleation and the dihedral angle. Theoretical prediction of the magnitude of the threshold stress is likely to be unreliable because of the uncertainty in the magnitude of the interface energies in ceramics, and because ceramics may already contain incipient cavities in the form of pores which have not been completely sintered during processing. However, experiments that have successfully demonstrated that polycrystalline ceramics can be superplastically deformed in uniaxial tension without fracture (Wang and Raj, 1984; Wakai et al., 1986) prove the existence of a threshold stress for cavity nucleation.

MEASUREMENTS OF THRESHOLD STRESS AND STRESS INTENSITY FACTOR

In this section experiments are proposed that can: (i) provide values for the threshold stress for cavity nucleation, (ii) prescribe the criterion for cavitation in multiaxial loading, and (iii) differentiate between the mode of fracture where failure occurs either by extensive cavitation or by propagation of crack from the surface.

The details of the experiment were described by Wang and Raj (1984). It consists of carrying out a uniaxial tensile test of a specimen inside a pressure vessel. The three principal stresses in the test are then $(\sigma - p_o)$, $-p_o$, and $-p_o$ where σ is the uniaxial stress, and p_o is the hydrostatic pressure. The maximum principal stress is then equal to $\sigma - p_o$; its magnitude can be varied by changing the hydrostatic pressure in the vessel. (Pressure vessels that can accommodate instrumentation and high temperature furnaces, and operate at pressures up to 200 MPa, are available.) By studying cavitation as a function of the maximum principal stress the threshold stress can be measured.

When an uncladded specimen is tested inside the pressure vessel, the hydrostatic pressure is effective only if the pores are physically separated from the pressurizing medium. Thus, surface cracks which can be penetrated by the pressurizing gas, feel the uniaxial stress in the same way as they would if the experiment was carried out at ambient pressure. To study the propagation of surface cracks under multiaxial loading, the specimen must be clad with an impermeable membrane. By studying the fracture behavior with and without the cladding, we can distinguish whether fracture is dominated by internal damage or by surface flaws.

In the superalloys literature, threshold stress intensity factor has been measured by measuring creep fracture lifetimes in specimens which are loaded to differing values of initial stress intensity factor (Sadananda and Shahinian, 1977; Pineau, 1985). An example, taken from Sadananda and Shahinian (1977), is reproduced in Fig. 12. Two points about this figure are interesting. First, the data give a natural asymptotic limit that can be safely assumed to be the threshold stress intensity factor. Second, it shows that the difference between the time for crack initiation and the total failure time is small; this gives support to the idea of using the threshold stress intensity factor as a design parameter.

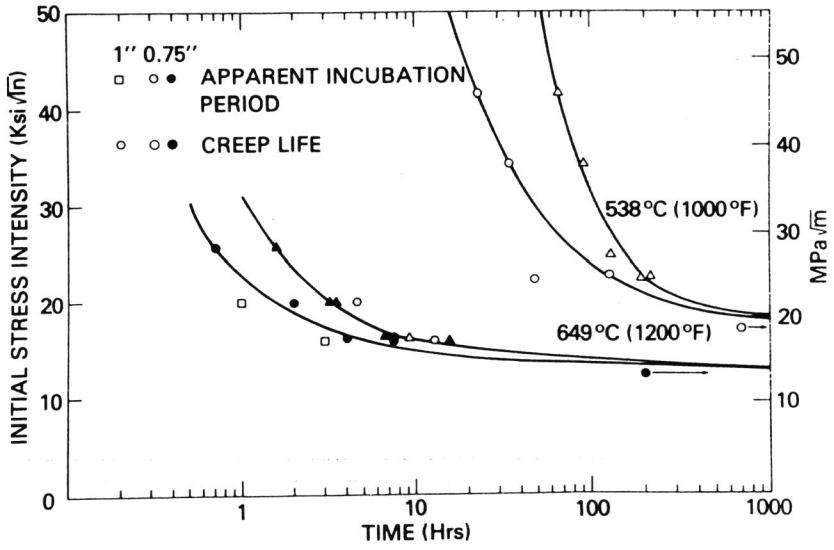

Fig. 12. Data for total lifetimes, and the time required for crack initiation in specimens of a nickel base superalloys that were loaded at different values of the initial stress intensity factor. Note that the lifetime is largely determined by the time for initiation. The asymptotic limit for the data gives a measurement of the threshold stress intensity factor (Sadananda and Shahinian, 1977).

CONCLUSION

A review of the literature has been presented to highlight the need for studying the threshold parameters for fracture in structural ceramics at high temperatures. Evidence is presented for the existence of a threshold stress intensity factor in experiments with silicon carbide and silicon nitride ceramics. Theoretical justification is given for the threshold stress and threshold stress intensity factor; it derives from the concept that nucleation of cavities is required for sub-critical fracture at high temperatures.

It is proposed that the threshold parameters can be measured through experiments that are carried out within a hydrostatic pressure. Other experiments, where lifetime of precracked specimens is measured are proposed for obtaining the threshold stress intensity factor.

Finally, it is concluded that the need for fundamental experimental work is greater than the need for theoretical modelling, at the present time.

ACKNOWLEDGMENTS

The work reported here summarizes the doctoral thesis research of Drs. J. Wang, R.K. Venkatachari, R.L. Tsai and P. Panda. Support from the Department of Energy, under Grants DE-EG77-S-02-4386 and DE-FG02-87ER45303 is very gratefully acknowledged.

REFERENCES

Davies, C.K.L. and S.K. Sinha Ray (1972). High Temperature Creep Deformation of Polycrystalline Alumina in Tension. In: Special Ceramics, (P. Popper, ed.), Vol. 5 pp. 193-209. British Ceramic Research Association, Stoke-on-Trent.

Evans, A.G. and S.M. Wiederhorn (1974). Crack Propagation and Failure Prediction in Silicon Nitride at Elevated Temperatures. J. Mater. Sci., 9, 270-278.

Evans, A.G. (1982). Consideration of Inhomogeneity Effects in Sintering. J. Amer. Ceram. Soc., 65, 497-501.

Frost, H.J. and M.F. Ashby (1982). Deformation Mechanism Maps. Pergamon Press, NY.

Fuller Jr., E.R., S.M. Wiederhorn, J.E. Ritter Jr. and P.B. Oates (1980). Proof Testing of Ceramics: Theory. J. Mater. Sci., 15, 2282-2295.

Gandhi, C., Fracture Mechanism Maps for Metals and Alloys. In: Flow and Fracture at Elevated Temperature (R. Raj, ed.). Amer. Soc. Metals, Metals Park, OH, pp. 83-119.

Interpretations of the ASME Boiler and Pressure Vessel Codes, Case 1592 (1974). American Society for Mechanical Engineers, New York.

Karunaratne, B.S.B. and M.H. Lewis (1980). High Temperature Fracture and Diffusional Deformation Mechanisms in Silicon Ceramics. J. Mater. Sci., 15, 449-462.

Kingery, W.D., H.K. Bowen and D.R. Uhlmann (1976). Introduction to Ceramics, 2nd ed., p. 808. John Wiley & Sons, New York.

Lange, F.F., B.I. Davis and D.R. Clarke (1980). Compressive Creep of Si_3N_4/MgO Alloys. J. Mater. Sci., 15, 601-610.

Marion, J.E., A.G. Evans, M.D. Drory and D.R. Clarke (1983). High Temperature Failure Cavitation in Liquid Phase Sintered Materials. Acta Metall., 31 [10] 1445-1457.

McHenry, K.D. and R.E. Tressler (1980). Fracture Toughness and High Temperature Slow Crack Growth in SiC. J. Amer. Ceram. Soc., 63 [3-4], 152-156.

Minford, E.J., and R.E. Tressler (1983). Determination of Threshold Stress Intensity for Crack Growth at High Temperature in Silicon Carbide Ceramics. J. Amer. Ceram. Soc., 66 [5], 338-340.

Nix, W.D. and J.C. Gibeling (1985). In: Flow and Fracture at Elevated Temperature (R. Raj, ed.), pp. 1-63. Amer. Soc. Metals, Metals Park, OH.

Pineau, A. (1986). Intergranular Creep Fatigue Crack Growth in Ni-Base Alloys. In: Flow and Fracture at Elevated Temperature (R. Raj, ed.), pp. 317-346. Amer. Soc. Metals, Metals Park, OH.

Pletka, B.J. and S.M. Wiederhorn (1982). A Comparison of Failure Predictions by Strength and Fracture Mechanics Techniques. J. Mater. Sci., 17, pp. 1247-1268.

Poteat, L.E. and C.S. Yust (1966). Creep of Polycrystalline Thorium Dioxide. J. Amer. Ceram. Soc., 49 [8] 410-414.

Raj, R. (1978). Nucleation of Cavities at Second Phase Particles in Grain Boundaries. Acta Metall., 26, 995-1006.

Raj, R. and S. Baik (1980). Creep Crack Propagation by Cavitation Near Crack Tips. Metal Sci., 14 [8-9], 384-394.

Raj, R. (1981). Morphology and Stability of the Glass Phase in Glass Ceramic Systems. J. Amer. Ceram. Soc., 64 [5], 245-248.

Riedel, H. (1985). Creep Crack Growth. In: Flow and Fracture at Elevated Temperature (R. Raj, ed.), pp. 149-174. Amer. Soc. Metals, Metals Park, OH.

Ritter Jr., J.E., P.B. Oates, E.R. Fuller, Jr. and S.M. Wiederhorn, (1980). Proof Testing of Ceramics: Experiment. J. Mater. Sci., 15, 1175-1181.

Sadananda, K. and P. Shahinian (1977). Creep Crack Growth in Alloy 718. Metall. Trans. A, 8A, 439-449.

Tsai, R.L. and R. Raj (1982). Creep Fracture in Ceramics Containing Small Amounts of a Liquid Phase. Acta Metall., 30, 1043-1058.

Venkatachari, K.R. and R. Raj (1986). Superplastic Flow in Fine Grained Alumina. J. Amer. Ceram. Soc., 69 [2] 135-138.

Wiederhorn, S.M. (1967). J. Amer. Ceram. Soc., 50, 407.

Wiederhorn, S.M., E.R. Fuller Jr., J. Mandel and A.G. Evans (1976). An Error Analysis of Failure Prediction Techniques Derived from Fracture Mechanics. J. Amer. Ceram. Soc., 59 [9-10], 403-422.

Wiederhorn, S.M., and N.J. Tighe (1978). Proof Testing of Hot Pressed Silicon Nitride. J. Mater. Sci., 13, 1781-1793.

Wiederhorn, S.M. and N.J. Tighe (1983). Structural Reliability of Yttria-Doped Hot-Pressed Silicon Nitride at Elevated Temperatures. J. Amer. Ceram. Soc., 66 [12], 884-889.

Wiederhorn, S.M., B.J. Hockey, R.F. Krause, Jr., and K. Jakus (1986). Creep and Fracture of Vitreous-Bonded Aluminum Oxide. J. Mater. Sci., 21, 810-824.

Wakai, F., S. Sakaguchi and Y. Matsimo (1986). Superplasticity of Yttria-Stabilized Tetragonal ZvO_2 Polycrystals. Adv. Ceram. Mater., 1 [3], 259-263.

Wang, J.-G. and R. Raj (1984). Mechanism of Superplastic Flow in a Fine-Grained Ceramic Containing Some Liquid Phase. J. Amer. Ceram. Soc., 67 [6], 399-409.

Wang, J.-G. and R. Raj (1984). Influence of Hydrostatic Pressure and Humidity on Superplastic Ductility of Two β-Spodumene Glass Ceramics. J. Amer. Ceram. Soc., 67 [6], 385-390.